

Anisotropy of Si $K\beta$ Emission: Interference of Fluorescence X Rays

Y. Ma,¹ K. E. Miyano,² P. L. Cowan,^{3,*} Y. Aglitzkiy,⁴ and B. A. Karlin⁴

¹Physics Department, University of Washington, Seattle, Washington 98195
and Pacific Northwest Laboratories, Richland, Washington 99352

²Physics Department, Brooklyn College, Brooklyn, New York 11210

³Physics Division, Argonne National Laboratory, Argonne, Illinois 60439

⁴National Institute of Standards and Technology, Gaithersburg, Maryland 20899

(Received 18 July 1994)

The Si $K\beta$ emission spectra of silicon is shown to be *anisotropic* when excited with near threshold monochromatic x rays. This anisotropy is attributed to the interference of the fluorescence x rays emitted from the different Si atoms. This is a result of coherent excitation by the monochromatic photons and the coherent decay of core holes on different Si atoms.

PACS numbers: 78.70.Dm, 71.25.Rk

It has long been accepted that x-ray spectra of crystals of high symmetry are isotropic [1]. This results from the general belief that core electrons involved in the x-ray transitions are localized on individual atoms and, consequently, x-ray absorption and the emission process occurring on those individual atoms are not correlated. Thus the absorption and emission spectra measures the unoccupied and occupied density of states, respectively. Here we present $K\beta$ emission spectra of silicon in the diamond structure, obtained with monochromatic photon excitation near the K absorption threshold, that show remarkable dependence on the crystal orientation. The anisotropy demonstrates the *interference* of fluorescence x rays emitted from individual Si atoms which is a result of *coherent* excitation and radiative decay of core levels. The correlated excitation and decay of core levels has many important implications on secondary spectroscopies including the recently observed excitation energy dependence in x-ray emission spectra [2–5]. It opens the way for performing *momentum resolved* absorption and emission spectroscopies and to use them for band structure determination. This technique of bandmapping has many useful properties that are complementary to the usual technique of angle resolved photoemission spectroscopy [6].

The experimental setup is shown in Fig. 1. The incident x-ray photons were provided by the beamline X24A of the National Synchrotron Light Source, using a pair of InSb crystals as the monochromator [7]. The Si $K\beta$ emission spectra were obtained using a spectrometer based on a bent InSb crystal and a position sensitive proportional counter (PSPC) [8]. The energy calibration of the spectrometer is done using the elastically scattering x rays, with the Si K -edge set at 1840 eV. The energy resolutions of the beamline monochromator and the fluorescence spectrometer are 0.8–1.0 eV.

To study the emission anisotropy, lacking an angle resolved x-ray spectrometer, we used silicon crystals of (100), (110), and (111) orientations. Care was taken to measure these samples under identical experimental con-

ditions. The Si(100), (110), and (111) samples were measured separately by translating them in and out of the incident beam while maintaining all the experimental settings, including the incident photon energy, the incidence and emission angles, and the spectrometer settings. This is done to ensure that there are no changes in geometrical conditions which could cause spurious changes in the emission spectra because of the sampling depth and the effective source size for the spectrometer.

In Fig. 2 we show the Si K -edge absorption and the $K\beta$ emission spectra. The emission spectra were obtained at several excitation energies. The absorption spectra were taken using the total electron yield method. Within experimental errors, the absorption spectrum in Fig. 2(a) was the same for all three crystals, and the emission spectra in Fig. 2(b) excited with photon energies high above the absorption edge are also independent of the crystal orientations. These observations are consistent with the traditional two-step, “absorption-followed-by-emission,” picture [1,9], where the absorption and emission processes are independent of each other and probe the unoccupied and occupied Si $3p$ -type density of states, respectively. Since the Si $1s$ electron is localized, the emitted x ray is regarded as coming from individual atoms and as incoherent. Because of the high symmetry of the diamond structure and

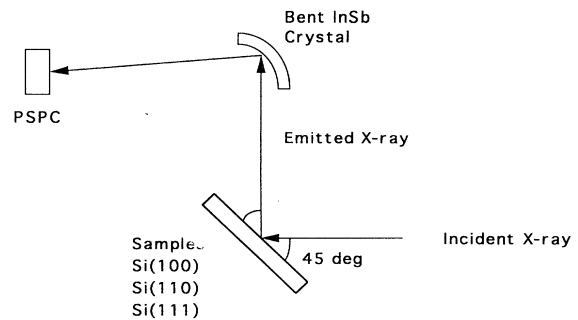


FIG. 1. Schematics of the experimental setup. PSPC stands for position sensitive proportional counter.

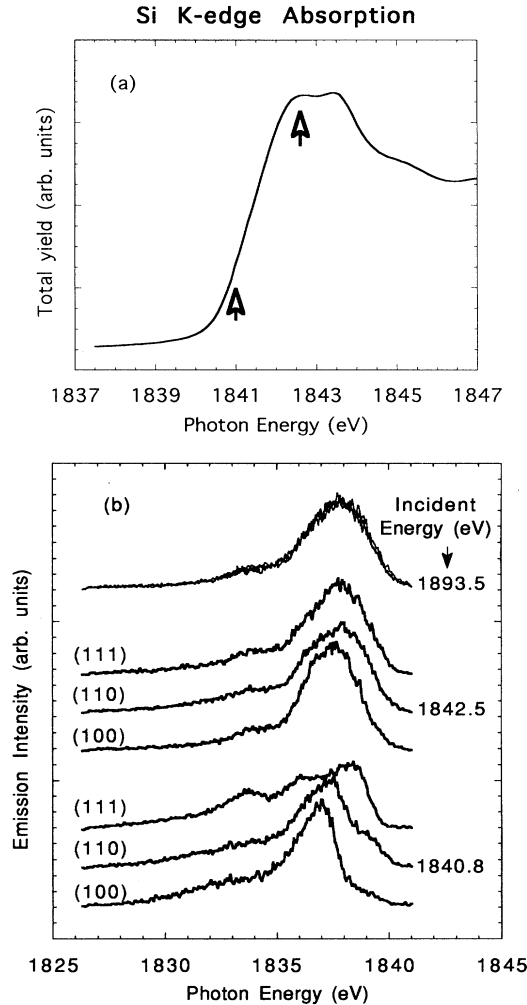


FIG. 2. Si K -edge absorption (a) and emission (b) spectra. The arrows in (a) indicate two of the photon energies used to obtain the emission spectra in (b). The $K\beta$ emission spectra for the three samples were taken at an excitation energy of 1895 eV (top, with three curves overlapped), 1842.5 (three curves in the middle), and 1840.8 eV (bottom). The emission spectra were normalized to have unit area.

the dipole transition selection rule, no emission anisotropy and no excitation energy dependence were expected.

Contrary to this conventional view, for near-threshold excitations, the emission spectra show strong crystal orientation dependencies. The spectral line shape also changes strongly with the incident energy. Since, except for the crystal orientations, these spectra were taken under identical experimental conditions, including the excitation energy, the polarization directions, the detection angle, and the spectrometer settings, the changing spectral shape cannot be due to experimental artifacts. Nor can it be explained by polarization effects such as the alignment of molecules in the excited states by polarized incident x rays [10].

The anisotropy can be attributed to the wave nature of the x rays and the *coherence* between the absorption and emission processes. Specifically, the fluorescence x-ray waves from different Si atoms *interfere* to give Bragg-like diffraction effects [11–13]. This phenomenon is best illustrated using the well known case of anomalous *elastic* x-ray scattering. The incident x ray excites a core electron into a previously unoccupied state and this photoelectron consequently recombines with the core hole to emit a secondary x-ray photon. The excitation-recombination processes on different atoms are coherent and, as a result, the emitted x-ray wave interferes to give the usual Bragg diffraction. This process is described by the Kramers-Heisenberg formula [14]:

$$\frac{d\sigma}{d\Omega} \propto \left| \sum_I \frac{\langle B | \mathbf{p} \mathbf{A}_2 | I \rangle \langle I | \mathbf{p} \mathbf{A}_1 | A \rangle}{E_I - E_A - \hbar\omega - i\Gamma/2} \right|^2, \quad (1)$$

where the intermediate states I correspond to the states with the core hole localized on each of the individual Si atoms. For elastic scattering the initial and final state of the sample are the same, $B = A$.

In the emission process we studied, the core hole is filled by a valence electron and the emitted x ray has different energy than the incident x ray. It is an inelastic process, $B \neq A$. Clearly this change does not affect the coherence of the core level excitation among the Si atoms and *all the decay processes that result in the same final state should be coherent* and the emitted x rays interfere [13]. In other words, as long as we cannot determine which atom has gone through the excitation-decay process, the emitted x ray from different Si atoms should interfere. This is the same as in the classical Young's double-slit experiment [15] where the basic requirement, as a result of the uncertainty principle, for the existence of the interference is that we cannot determine the path of the waves. Since the electron-hole pair in the final state of our experiment occupies the conduction-valence band states and is delocalized, this condition for the interference is satisfied. The interference of the fluorescence x ray yields a Bragg-like diffraction condition which relates the momentum of the x-ray photons to that of the electron-hole pair in the final state.

It can be easily shown that this quasi-Bragg condition can be equivalently derived from the Si band structure [16] picture illustrated in Fig. 3. The key here is the *coherence* between the absorption and emission processes that makes it possible to use the Bloch wave function for the core state which is simply a superposition of core wave functions localized on individual atoms. In the excitation process, the incident photon excites a Si $1s$ electron into the conduction band. The energy $\varepsilon_e(\mathbf{k}_e)$ and the crystal momentum \mathbf{k}_e of the photoelectron is determined by the energy relation $\varepsilon_e(\mathbf{k}_e) - \varepsilon_{1s} = \hbar\omega_1$. A virtual core hole is created with momentum $\mathbf{k}_{ch} = \mathbf{q}_1 - \mathbf{k}_e$. In the radiative decay process a valence electron from $\mathbf{k}_h = \mathbf{q}_2 - \mathbf{k}_{ch}$ fills the core hole. The overall process

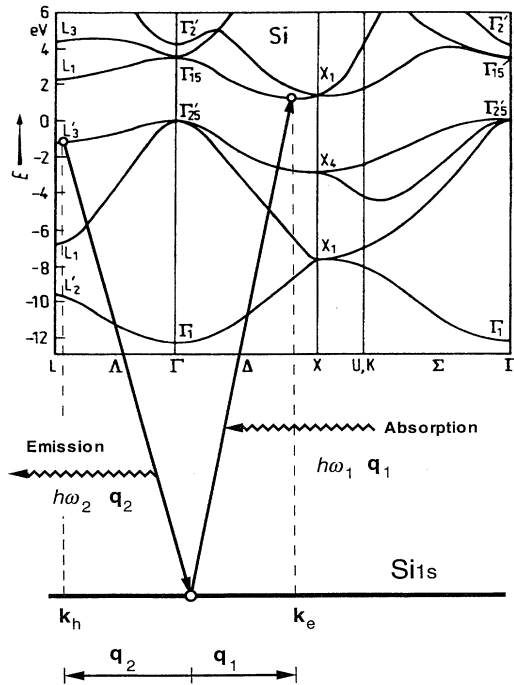


FIG. 3. Illustration of the XRIS process using the band structure of silicon. \mathbf{q}_1 and \mathbf{q}_2 are the momentum of the incident and emitted x rays, respectively. \mathbf{k}_e and \mathbf{k}_h are the momentum of the photoelectron in the conduction band and the valence electron.

produces a momentum conservation relation, $\mathbf{q}_1 - \mathbf{q}_2 = \mathbf{k}_e - \mathbf{k}_h + \mathbf{G}$, which is the modified Bragg condition.

This interference effect, which can be more generally called x-ray resonant inelastic scattering (XRIS) [11], will produce anisotropy in the emission experiment. For a given excitation energy $\hbar\omega_1$, the momentum of the photoelectron \mathbf{k}_e is limited to certain values by a given band structure, and the momentum of the valence hole created in the emission process will vary as the incident direction (\mathbf{q}_1) and/or the detection direction (\mathbf{q}_2) is changed. Consequently, the emission spectra taken in different directions will be different. This is confirmed in Fig. 2(b). In the following we offer a qualitative interpretation of the anisotropy of the spectra excited with incident energy of 1840.8 eV in Fig. 2(b).

The inelastic scattering picture also offers a natural explanation for the excitation energy dependence of the spectral line shape [2-5]. The momentum of the electron in the final state is a function of the incident photon energy through the energy relation, $\varepsilon_e(\mathbf{k}_e) - \varepsilon_{1s} = \hbar\omega_1$. Since only emission from $\mathbf{k}_h = \mathbf{q}_2 - \mathbf{q}_1 + \mathbf{k}_e$ and $\varepsilon_h(\mathbf{k}_h) = \varepsilon_{1s} + \hbar\omega_2$ of the valence band is allowed, as the incident energy $\hbar\omega_1$ is varied, the emission spectral line shape will also vary, with enhanced emission from a region or regions of the Brillouin zone (BZ) determined by the energy and momentum conservation. The

previous experiments [2-5] were done in the soft x-ray region where the momentum transfer from the x-ray photons is small compared to the size of the Brillouin zone, so that the absorption/emission transitions participating in the scattering process could be considered to be nearly vertical on a band structure diagram such as Fig. 3. In these cases no emission anisotropy is expected.

In our experiment, \mathbf{q}_1 and \mathbf{q}_2 are fixed relative to each other. The momentum transfer $\mathbf{q}_2 - \mathbf{q}_1$ is along the (100), (110), and (111) directions for the three samples. So, the direction of the momentum transfer changed for different samples. For the near threshold excitation of 1840.8 eV, the photoelectron is excited to the conduction band minimum near the X_1 point at about $\Delta_1 = 2\pi/a(0.8, 0, 0)$, where $a = 5.43 \text{ \AA}$ is the lattice constant of Si. The momentum conservation then predicts that the emission can only occur from the regions in the BZ determined by $\mathbf{k}_h = \Delta_1 + (\mathbf{q}_2 - \mathbf{q}_1)$. For the (111) sample, it can be shown that for the six points evaluated according to the above relation three of them are very close to the L point and three close to the K type of critical points. Indeed, the most pronounced peaks of the bottom curve in Fig. 2(b) are at approximately $-7, -4.5, -2 \text{ eV}$, which correspond to the calculated positions of the $L_1, K_4,$ and L_3 points. Similarly for momentum transfer along (110) direction, the maximum intensity is predicted to occur near the X and Γ points. In Fig. 2(b) the maximum of the Si(110) spectrum is indeed at about the X_4 points. We even notice enhanced emission near the top of the valence band Γ_{25} , where no emission intensity is normally observed due to the near zero density of states. For the (100) crystal, the XRIS theory predicts enhanced emission near the $X, \Gamma,$ and also the W points, and that appears to indeed be the case in Fig. 2(b). At high excitation energies, the photoelectron is excited into free-electron-like states. The electron momentum can take essentially any value due to the folding of the bands into the first Brillouin zone. Consequently, as shown in Fig. 2(b) the anisotropy disappeared for the spectra excited with 1895 eV photons.

The emission anisotropy has been explained by the interference of the fluorescence x rays. Using a spectrometer capable of continuously varying the angle of detection, we should be able to map the valence band. This is a new technique for determining the band structure of solids, which has several properties that are complementary to the traditional angle resolved photoelectron spectroscopy, including the bulk sensitivity and the elemental, orbital as well as the chemical sensitivity. The limitations include the requirement of appropriate core levels so that the x-ray wave vectors match that of the BZ of the materials being studied. In addition, the inelastic scattering picture only works near the threshold. Away from the threshold, the lifetime effect of the final state and other many-body interactions could destroy the coherence [13].

We note that the coherent excitation and decay is a general phenomena and is not restricted to x rays. For

example, we expect core-valence-valence Auger spectra excited with monochromatic x rays or electrons to exhibit similar interference effects. The effects will be more complex due to the extra electron involved and the Coulomb interaction that governs the Auger process.

Finally, it is well known from the optical theorem that the x-ray absorption is proportional to the forward elastic scattering amplitude. Thus one can expect to obtain information beyond those obtained from the x-ray absorption experiment if one goes to off-forward scattering geometry and to inelastic scattering measurements. This experiment as well as the recently discovered diffraction anomalous fine structure (DAFS) [17] demonstrated this principle.

In summary, we have shown that despite their localized nature, core level absorption and the emission process are intrinsically collective phenomena. Whether these collective effects can be seen or not depends on the final state of the system, i.e., method of detection. They can be seen only if the measurement results in delocalized final states. The existence of the coherence in the excitation and decay processes will have broad implications in synchrotron radiation spectroscopies, including the possibilities for electronic momentum resolved x-ray spectroscopy.

We acknowledge useful discussions with M. Blume and E. A. Stern. The National Synchrotron Light Source is operated under contract from DOE.

*Deceased.

[1] See, e.g., M. Born and E. Wolf, *Principles of Optics*

(Pergamon, Oxford, 1980); B.K. Agarwal, *X-ray Spectroscopy* (Springer-Verlag, Berlin, 1991).

- [2] Y. Ma *et al.*, Phys. Rev. Lett. **69**, 2598 (1992).
 [3] K.E. Miyano *et al.*, Phys. Rev. B **48**, 1918 (1993).
 [4] P.D. Johnson and Y. Ma, Phys. Rev. B **49**, 5024 (1994).
 [5] P. Skytt *et al.*, Phys. Rev. B **50**, 10457 (1994).
 [6] See, e.g., *Angle-Resolved Photoemission*, edited by S.D. Kevan (Elsevier, Amsterdam, 1992).
 [7] P.L. Cowan *et al.*, Nucl. Instrum. Methods Phys. Res., Sect. A **246**, 154 (1986).
 [8] S. Brennan, P.L. Cowan, R.D. Deslattes, A. Henins, D.W. Lindle, and B.A. Karlin, Rev. Sci. Instrum. **60**, 2243 (1989).
 [9] See, e.g., P. Eisenberger, P.M. Platzman, and H. Winick, Phys. Rev. Lett. **36**, 623 (1976).
 [10] S.E. Southworth *et al.*, Phys. Rev. Lett. **67**, 1098 (1991); D.W. Lindle *et al.*, Phys. Rev. Lett. **60**, 1010 (1988).
 [11] Y. Ma, Phys. Rev. B **49**, 5799 (1994).
 [12] P. Nozieres and E. Abrahams, Phys. Rev. B **10**, 3099 (1974); H. Kh. Gel'mukhanov, L.N. Mazalov, and N.A. Shklyeva, Sov. Phys. JETP **44**, 504 (1977).
 [13] Y. Ma and M. Blume, in Proceedings of International Conferences on Synchrotron Radiation Instrumentation (SRI-94) [Rev. Sci. Instrum. (to be published)].
 [14] See, e.g., J.J. Sakurai, *Advanced Quantum Mechanics* (Addison-Wesley, Reading, MA, 1967), Chap. 2.
 [15] See, e.g., R.P. Feynman, R.B. Leighton, and M. Sands, *The Feynman Lectures on Physics* (Addison-Wesley, Reading, MA, 1965), Vol. 3.
 [16] See, e.g., J.R. Chelikowsky and M. Cohen, Phys. Rev. B **10**, 5095 (1974).
 [17] H. Stragier *et al.*, Phys. Rev. Lett. **69**, 3064 (1992).